91602
new 82-10 LEGAL NOTICE

This report was prepared by Ontario Hydro and, while effort has been made to assure the accuracy and applicability of the material contained herein, neither Ontario Hydro nor any person acting on its behalf:

(a) makes any warranty, express or implied with respect to the use of any information, apparatus, method or process disclosed in this report or that such use may not imringe privately owned rights; or

(b) assumes any liabilities with respect to the use of, or for damages resulting from the use of, any information, apparatus, method or process disclosed in this report.

ontario hydro
research division

COMPLIMENTARY COPY
Please Credit Ontario Hydro Research if Reproduced in Whole or in Part

ELECTROCATALYTIC, SURFACE AND SEMICONDUCTING PROPERTIES OF REACTIVELY SPUTTERED COBALT OXIDE

Report No 89-114-K

L.C. Schumacher
Chemist
Process Chemistry Section
Chemical Research Department

ABSTRACT

Cobalt oxide films, fabricated by reactive sputtering in a 100% pure 0_2 plasma are highly nonstoichiometric with a bulk oxygen to cobalt ratio of ~1.15. Conversely, surface XPS studies indicate an oxygen to cobalt ratio ranging from 1.8 - 3.0 and show the presence of Co^{+3} only in the surface region of the as formed films. Infrared and Raman spectra however confirm the presence of both Co^{+3} and Co^{+2} in the bulk and indicate that these highly defective films possess the spinel structure. Photoelectrochemical and impedance studies show that the sputtered oxide is a highly doped p-type semiconductor with an indirect bandgap of E_g ~1.50 eV. The electrocatalytic properties of these oxide films for oxygen reduction and evolution are reported.

job	file	date	report no.
31-511-011	826.7	July 19, 1989	89-114-K

91602
new 82-10

89-06329/

ontario hydro
research division

EXECUTIVE SUMMARY

ELECTROCATALYTIC, SURFACE AND SEMICONDUCTING PROPERTIES OF REACTIVELY SPUTTERED COBALT OXIDE

L.C. Schumacher
Process Chemistry Section
Chemical Research Department

The development of efficient and stable aqueous O_2 reduction electrocatalysts based on mixed metal oxides requires that the oxide: 1) possess a metal species exhibiting redox levels in the vicinity of the O_2/OH^- reversible potential and 2) be able to support high anion vacancy concentrations which will contribute to high anion mobilities through the oxide. Fabrication procedure plays an important role in this regard since those synthesis techniques which give rise to high defect concentrations will be preferable over those which give highly crystalline, stoichiometric oxides. Much of the variability observed with electrocatalysts is attributable to variations in surface/bulk properties arising from different fabrication methods. Atomic sputtering is a very flexible thin film deposition technique which is being employed to produce mixed metals and mixed metal oxides being screened as O_2 reduction catalysts. Cobalt oxide, which possesses a redox couple Co^{+2}/Co^{+3} ~200 mV negative of the O_2/OH^- couple is being studied first as a simple oxide and will subsequently be mixed with other components such as Nd, Sm and Bi, to mention a few.

Cobalt oxide films, fabricated by reactive sputtering in a 100% pure O_2 plasma are highly nonstoichiometric with a bulk oxygen to cobalt ratio of ~1.15. Conversely, surface XPS studies indicate an oxygen to cobalt ratio ranging from 1.8 - 3.0 and show the presence of Co^{+3} only in the surface region of the as formed films. Infrared and Raman spectra confirm the presence of both Co^{+3} and Co^{+2} in the bulk and indicate that these highly defective films possess the spinel structure. Photoelectrochemical and impedance studies show that the sputtered oxide is a highly doped p-type semiconductor with an indirect bandgap of E_g ~1.50 eV.

job	file	date	report no.
31-511-011	826.7	July 19, 1989	89-114-K

CONTENTS

		Page
1.	INTRODUCTION	1
2.	EXPERIMENTAL	1
3.	RESULTS AND DISCUSSION	3
	3.1 Solid State and Semiconducting Properties	3
	3.2 Electrocatalytic Properties	4
4.	CONCLUSIONS	6
5.	ACKNOWLEDGEMENT	7
6.	SUGGESTIONS FOR FUTURE WORK	7
REFERENCES		8
FIGURES		9
DISTRIBUTION		last page

LIST OF FIGURES

		Page
1.	X-ray diffraction spectra for a) ~1000 Å cobalt oxide sputter deposited directly onto pyrex, b) ~1000 Å cobalt oxide deposited on ITO and c) ITO on pyrex.	9
2.	XPS spectra of cobalt metal and several cobalt oxide species, from reference 8.	10
3.	Infrared spectrum of ~1000 Å cobalt oxide sputter deposited onto silicon substrates.	11
4.	Raman spectrum of ~1000 Å cobalt oxide film deposited onto ITO, a) before potential scanning to -0.90 V (SCE) and b) after potential scanning to -0.90 V (SCE).	12
5.	AC white light cathodic photoresponse demonstrating p-type semiconducting nature of these cobalt oxide films.	13
6.	AC quantum efficiency measured with electrode held under -0.70 V(SCE) bias.	14
7.	Indirect bandgap determination of sputtered cobalt oxide obtained from quantum efficiency data of Fig. 6.	15
8.	Mott-Schottky plot at 10^3 Hz extrapolating to V_{fb} ~ -0.10 V(SCE).	16
9.	Energy level diagram showing the position of the OH^-/O_2 and H^+/H_2 redox levels relative to the conduction and valence bands of the cobalt oxide, constructed using experimentally determined values for E_g and V_{fb}.	17
10.	Mott-Schottky plots for a) cobalt oxide films deposited and vacuum annealed 8 hours at 300°C and b) cobalt oxide deposited at room temperature.	18
11.	Cyclic voltammogram of sputtered cobalt oxide between the potential limits initially a) -0.60 to 0.6 V (SCE) and then b) -0.90 to 0.60 V (SCE).	19
12.	Capacitance of electrode of Fig. 11, 1- before and 2- after potential cycling to -0.90 V (SCE) corresponding to a change from a smooth to rougher morphology film.	20
13.	O_2 reduction currents at rotating ring disc electrode. Cobalt oxide ~1000 Å sputter deposited onto stainless steel disc, area = 0.196 cm^2. Ring current at ~3000 rpm negligible.	21

LIST OF FIGURES (Con't)

		Page
14.	Plot of I^{-1} vs $(\omega)^{-1/2}$ for O_2 reduction on cobalt oxide film deposited and vacuum annealed at ~300°C.	22
15.	Tafel plots for O_2 evolution at room temperature of sputtered cobalt oxide deposited on ITO.	23

ontario hydro
research division

To

Dr. D. Mills
Director of Research

ELECTROCATALYTIC, SURFACE AND SEMICONDUCTING
PROPERTIES OF REACTIVELY SPUTTERED COBALT OXIDE

1. INTRODUCTION

The cobalt containing defect perovskites (eg. $La_{1-x}\ Sr_x\ CoO_3$) are one class of nonstoichiometric oxides which have shown high activity as aqueous O_2 reduction electrocatalysts in alkaline media (1-6). While reasonable behaviour with porous gas diffusion electrodes has been obtained, problems with low oxide conductivity and poor mass transport remain. Consequently, the true electrocatalytic properties of these oxides is yet to be determined. To address this issue, atomic sputtering will be employed to produce several ternary mixed oxides containing cobalt, and the semiconducting and electrocatalytic properties of these systems determined. Before doing this however, it is necessary to characterize the surface, and the electrocatalytic and semiconducting properties of sputtered cobalt oxide by itself, as the simple oxide (when doped) is a good O_2 reduction/evolution catalyst. The results of such a study are presented in this report.

2. EXPERIMENTAL

Cobalt oxide was deposited from a 6" diameter cobalt metal target (Metron) 99.9% pure. The oxide was obtained by deposition in a 100% O_2 plasma at 10 microns chamber pressure. The pure O_2 plasma was employed to ensure that Co_3O_4 was obtained, as previous studies of sputtered cobalt oxide indicate that for a plasma containing both Ar and O_2, films of variable metal (cobalt) to oxygen ratios are obtained, this ratio being a function of the O_2 partial pressure and flow rate (7).

All photoelectrochemical studies were carried out at room temperature, $22^o \pm 2^oC$ and usually in 0.10 M NaOH except where otherwise noted. The sodium hydroxide was analytical reagent grade, the water was triply distilled and

nitrogen purged for 30 minutes before electrochemical studies began. An SCE electrode was used as reference. Photoelectrochemical studies were made using a Princeton Applied Research (PAR) Model 170 Electrochemistry System in conjunction with a 150W high pressure xenon arc lamp. AC photocurrents were obtained using a mechanical chopper (40Hz) and a phase sensitive amplifier. Impedance measurements were made using a PAR dual-phase, phase-sensitive amplifier, Model 129A. The AC signal (3 mV peak-peak) was provided by a Wavetek Model 182A function generator. The phase of the lock-in amplifier was referenced against the AC voltage across the cell and the in- and out-of-phase components of the cell current were measured via a standard 10 ± 0.005% Ω resistor in series with the cell.

Action spectra were obtained using a Spex Minimate monochromator and a 150 W xenon light source. AC quantum efficiencies, ϕ, were calculated using the expression $\phi = 1.2408J/I_o\lambda$, where J is the photocurrent density in microamperes per square centimeter, 1.2408 is a conversion factor relating photon flux density to power flux density, and I_o is the incident power flux density in milliwatts per square centimeter at wavelength λ (expressed in nanometers).

Oxygen reduction studies were performed with a Pine Instruments RDE4 potentiostat along with a demountable rotating ring disc (area=0.196 cm^2) assembly employing a gold ring. The reference electrode was the Hg/HgO system with a high purity spectroscopic grade carbon rod used as the counter electrode. The O_2 saturated electrolyte was 0.10 M KOH (analytical grade) with the water purified using a Zenopure Laboratory Water System Ultra 70 ASPM type grade water. ITO (Indium Tin Oxide) and stainless steel exhibit high activation overpotentials for both O_2 evolution and reduction respectively and hence are not expected to contribute directly in any significant way to the electrocatalytic behaviour of the overlaying films.

Raman spectra were recorded using a Dilor OMARS89 microprobe with a x100 objective. Excitation was achieved using the 514.5 nm line of a Coherent Radiation Innova 70 argon ion laser. X-ray photoelectron spectra were obtained with a Surface Science 5 x 100 spectrometer.

3. RESULTS AND DISCUSSION

3.1 Solid State and Semiconducting Properties

X-ray diffraction spectra of reactively sputtered cobalt oxide deposited on Pyrex exhibit some peaks attributable to Co_3O_4. Deposition onto ITO substrates results in strong orientation affects, as is evident from Fig. 1. Surface compositional analysis of the as sputtered oxide films, based on the XPS studies, reveals an oxygen to cobalt ratio varying from O/Co ~ 1.8 - 3.0. On the other hand compositional analysis from auger depth profile studies gave a bulk oxygen to cobalt ratio of O/Co ~1.15 which was approximately constant throughout the bulk of the ~1000 Å thick film. This oxygen to cobalt ratio is significantly less than 1.33 which would be expected for fully stoichiometric Co_3O_4, suggesting these films are nonstoichiometric by virtue of oxygen deficiency. The conductivity of cobalt oxide films sputter deposited at ~300°C and vacuum annealed were of the order of ~10^{-3} Ω^{-1}-cm^{-1} while films deposited at room temperature exhibited conductivities ~2 Ω^{-1}-cm^{-1}. In Fig. 2 the XPS spectrum of the as sputtered cobalt oxide is compared to previously reported spectra for various cobalt species (8). The lack of a broad shoulder centered at ~786 eV for the sputtered oxide compared to Co_3O_4 and Co^o suggest the absence of Co^{+2} in the surface region of these oxide films. Annealing the as formed sputtered films in both O_2 and vacuum at ~ 300°C led to the same surface cobalt species but a variable O/Co ratio. The IR spectrum consisted of four sharp peaks at 660 cm^{-1}, 562 cm^{-1}, 386 cm^{-1} and 220 cm^{-1} while the Raman spectrum measured between 350 - 880 cm^{-1} consisted of four sharp peaks centered at 684, 614, 620 and 477 cm^{-1}, compare Fig. 3 and 4a. While the crystal structure cannot be determined from XRD studies, the presence of the four IR bands is characteristic of the spinel structure, Co^{II} (Co_2^{III} O_4). The two higher IR frequency components at 660 cm^{-1} and 562 cm^{-1} are attributed to vibrations of the octahedrally coordinated Co^{III} (9). Of the lower frequency components, that at 386 cm^{-1} is found to depend on both bi-and trivalent cations in the lattice while the peak at 220 cm^{-1} depends only on the tetrahedrally coordinated Co^{II} cation. Since Co_3O_4 is a normal spinel, all the Co^{II} are tetrahedrally coordinated. The complimentary nature of the Raman and IR bands is typical of the normal spinels belonging to the symmetry group O^7_h and possessing a centre of symmetry.

The cathodic white light photoresponse of Fig. 5 shows these films to be p-type. The optical transition giving rise to the photogenerated minority electrons is indirect as deduced from the linear plot of $(\phi h\nu)^{1/2}$ vs $h\nu$, see Fig. 7. The energy gap is extrapolated from the intercept of the linear region with the energy axis to give E_g ~ 1.50 eV and corresponds to the

crystal field transition $^1A_1$ - $^1T_1$ of octahedrally coordinated Co^{+3}(10). The low quantam efficiencies of these films are typical of low mobility oxides where carrier transport is by a hopping mechanism.

The flatband potential, V_{fb}, of the sputtered cobalt oxide was determined using impedance spectroscopy and V_{fb} ~ -0.10V (SCE), this being extrapolated from the linear portion of the Mott-Schottky plot (10^3Hz) of Fig. 8. From the slope of the linear portion and assuming a dielectric constant of K ~ 10(10) gives a doping density of $N_d \sim 6.5 \times 10^{21}$ cm^{-3}.

The Mott-Schottky plots of Fig. 10 show the effect of film preparation procedure on the impedance properties of the oxide. Fig. 10a is the plot for a film deposited and vacuum annealed at ~300°C while Fig. 10b is for a film reactively sputtered at room temperature. This latter type of film gave the poorest O_2 reduction behavior while the former type consistently gave the best. The low quantum efficiencies are to be expected in view of the high doping density exhibited by these nonstoichiometric films and that the minority carriers move via a hopping mechanism, this due to the weakly overlapping cobalt based d-orbitals which form the valence and conduction bands (12). As well, the electron diffusion length will be less than the Debye length due to high recombination rates arising from the high doping density, N_d. Hence, $L_n \leq (\varepsilon\varepsilon_o kT/e^2N_d)^{1/2} \sim 3$ Å, where ε_o is the permittivity of free space, e the charge on the electron, ε the relative dielectric constant and k Boltzman's constant.

The low bulk oxygen to cobalt ratio, ~1.15, (reproduced with several samples) is significantly lower than for the fully stoichiometric oxide where O/Co=1.33 formed by atomic sputtering in an oxygen-argon plasma (7). On the other hand, films of nonstoichiometric Co_{3-x} O_4 grown by decomposition of cobalt nitrate have been reported as being metal deficient (13). The oxygen deficient sputtered films of this study are stable in both atmosphere and under oxygen evolution conditions.

3.2 Electrocatalytic Properties

The cyclic voltammogram for a film sputter deposited at 250°C and scanned between -0.60 to 0.60 V (SCE) is essentially featureless, see curve 1 of Fig. 11. No change in the CV was observed after evolving oxygen for 3 hrs at 1 mA-cm^{-2} current density. When the cathodic potential limit was extended to -0.90 V (SCE), a significantly different voltammogram was obtained as seen in curve 2 of Fig. 11. SEM studies of sputtered cobalt oxide films deposited on ITO both before and after potential scanning to -0.90 V (SCE) indicates a

significant amount of roughening is occurring. A roughness factor of ~1.5 - 1.8 is estimated from the capacitance data obtained before and after potential cycling to -0.90 V (SCE), see Fig. 12.

In addition to roughening the film, potential scanning to -0.90 V (SCE) also results in the incorporation of hydroxide species in the surface region, as evidenced from the XPS studies. Angular dependent XPS studies show the existence of cobalt hydroxide species to at least a depth of ~40 Å. However, no O-H stretching mode was detectable in the ex-situ Raman studies, so the total hydroxide content is assumed to be low. Ex-situ Raman studies of these films on ITO reveal that both before and after cycling to -0.90 V (SCE) similar bands are observed; however, cycling led to a shifting of all the peaks by 5 to 8 cm^{-1} to lower frequencies and an approximately 50% increase in the bandwidths, see Fig. 4. This behaviour is consistent with increased disorder in the film. Nonstoichiometric oxide was also produced by thermal decomposition of cobalt (II) nitrate at 300°C and also gave the same broadened and shifted Raman bands. These pyrolitic samples are reported as being cobalt deficient (13) while the electrochemically cycled films are oxygen deficient. The 676 cm^{-1} band of the electrochemically cycled film shows no evidence of a shoulder at 684 cm^{-1}, confirming that the entire film has been perturbed. Ex-situ Raman studies of anodically grown cobalt oxide films behaved differently with the reduction of the oxide occurring at ~-0.4V (SCE), resulting in the loss of all the Raman peaks (14).

Rotating disc currents as a function of disc potential for O_2 reduction are shown in Fig. 14 at several rotation speeds. No ring current was observed in this same potential region, suggesting solution free peroxide is not produced. The lack of a diffusion limited current indicates that the O_2 reduction reaction is under kinetic control over the entire potential region. The linearity of the I^{-1} vs $(\omega)^{-1/2}$ plot, see Fig. 14, indicates that the kinetics of the O_2 reduction are first order with respect to dissolved O_2, this based on the expression (14) $\frac{1}{I} = \frac{1}{I_k} + \frac{1}{B\sqrt{\omega}}$. The inverse of the slope of this plot at -0.70 V (Hg/HgO) gives B 0.016 mA/$(rpm)^{1/2}$, which, using the expression for B given by Newman (16) in conjunction with the solubility and diffusion coefficient data of Gubbins et al (17), gives ~3.7 electrons transferred for each oxygen molecule crossing the diffusion layer. Potential scanning to the region negative of -0.80V (Hg/HgO) resulted in irreversible degradation of the O_2 reduction currents.

The Tafel plots for O_2 evolution of the sputtered cobalt oxide on ITO, at room temperature is shown in Fig. 15, before cathodic polarization to -0.90V (SCE). While potential cycling to -0.9V (SCE) resulted in irreversible decrease in the O_2 reduction current, the kinetics for oxygen evolution improved slightly

with a constant decrease in overpotential over several decades of current density, an improvement which can be partly attributed to the higher surface area of the roughened films.

Mechanistic studies on lithium doped Co_3O_4 and other cobalt containing mixed metal oxides such as $La_{1-X}Sr_XCoO_3$ indicate that increasing the concentration of Co^{+3} in the surface region results in significantly improved O_2 evolution kinetics (1-5, 18, 19). The reason is presumably that the preferred surface sites for adsorption of OH^- are the trivalent cobalt species. The Tafel slope of these sputtered films, ~50 mV/decade at room temperature is close to that reported for lithiated Co_3O_4 (60 mV/ decade) and $La_{0.8}Sr_{0.2}CoO_3$ (65 mV/decade) (18,1) suggesting that Co^{+3} are the active sites at the sputtered oxide surface. The increased overpotential for O_2 evolution displayed by these films relative to bulk Co_3O_4 and lithiated Co_3O_4 (18, 19) is due in part to the much lower surface area of the former over the latter. The geometric area of the uniform, flat sputtered films will be very close to the true surface area. A further contribution to the increased overpotential is the high O/Co surface ratio (1.8 - 3.0) observed with these films. In addition to decreasing the number of active sites for OH^- adsorption, the oxygen excess may contribute to the increased overpotential in another way. As pointed out earlier several mixed metal oxides possessing either the defect perovskite or pyrochlore structure have exhibited O_2 evolution/reduction kinetics comparable to or exceeding platinum. These oxides, in addition to exhibiting high electronic conductivities, possess exceptionally high oxide ion conductivities attributable to substantial oxygen vacancies capable of being induced and supported in the se highly defective crystal structures. These anion ion vacancies are thought to be partially responsible for the low overpotential for the oxygen reaction, probably by providing sites for hydroxide species uptake important in the oxide pathway mechanism of O_2 evolution while contributing to high oxide ion conductivity which is probably important in O_2 reduction. Considering that these sputtered cobalt oxide films are characterized by oxygen excess surface regions, the oxide mobility will likely be lower than for an anion deficient surface resulting in higher overpotentials for both O_2 reduction/evolution. In addition to this, it has been suggested that Co^{+3} sites are involved in the O_2 reduction reaction, acting as acceptor sites for electrons from the bulk and donor sites for O_2 molecules with the rate determining step being electron transfer to the molecule from the surface (20).

4. CONCLUSIONS

Reactively sputtered cobalt oxide films deposited between 200 - 300°C are duplex in nature displaying very different surface and bulk oxygen-to-cobalt ratios with the bulk being oxygen deficient and the surface oxygen excess.

Both ratios are far from O/Co = 1.33 expected for the normal stoichiometric spinel. IR and Raman spectra suggest a bulk spinel lattice is obtained so that these sputtered film are apparently highly defective. The bulk oxygen-to-cobalt ratio, O/Co ~ 1.15, is significantly less than that observed for other methods of growth, where it is generally $\geq$ 1.33. These sputtered films are p-type semiconductors with bandgaps in the vicinity of 1.5 eV. Low substrate temperatures (< 200°C) during film deposition adversely affects the kinetics for O_2 reduction.

5.0 ACKNOWLEDGMENT

The author would like to thank Mr. Ingo Holzhueter for carrying out some of the electrocatalytic studies and Mr. Brian Pattenden for the X-ray data.

6.0 SUGGESTIONS FOR FUTURE WORK

In order to produce an efficient bifunctional O_2 cathode with cobalt as one of the component will require mixing with another component which favours the trivalent state of cobalt and the creation of anion vacancies in the lattice. Codeposition of cobalt with metal species with large ionic radii such as Nd and Sm and La, or combinations thereof is one possible route to follow.

Approved by:

D.J.R. Dodd
Manager
Chemical Research Department

Prepared by:

L.C. Schumacher
Chemist
Process Chemistry Section
Chemical Research Department

Reviewed by:

S.H. Hawthorne
Acting Supervising Engineer
Process Chemistry Section
Chemical Research Department

LCS:fc

REFERENCES

1. Y. Matsumoto, H. Manabe, and E. Sato, J. Electrochem. Soc., 127, 811 (1980).

2. Y. Matsumoto, H. Yoneyama and H. Tamura, J. Electroanal. Chem., 79, 319 (1977).

3. D.B. Meadowcroft, Nature, 226, 847 (1970).

4. T. Kudo, H. Obayashi and M. Yoshida, J. Electrochem. Soc., 124, 321 1977.

5. T. Kudo, H.Obayashi and T. Gego, J.Electrochem. Soc., 122, 159 (1975).

6. H.S. Horowitz, J.M. Longo and H.H. Horowitz, J. Electrochem. Soc., 130, 1851 (1983).

7. J.B. Cook and M.P. Van Der Meer, Thin Solid Films, 144, 165 (1986).

8. N.S. McIntyre and M.G. Cook, Analytical Chemistry, 47, 2208 (1975).

9. J. Preudhommer and P. Tarte, Spectrochemica Acta, 27A, 1817 (1971).

10. J.W.D. Martens, W.L. Peeters, H.M. Van Noort, and M. Erman, J. Phys. Chem. Solids, 46, 411 (1985).

11. The Oxide Handbook, Ed. G.V. Samsonov, IFI/Plenum Data Corp. 1973.

12. J.M. Honig, "Electronic Band Structure of Oxides with Metallic or Semiconducting Characteristics" in Studies in Physical and Theoretical Chemistry, Vol. 11A, p 1-96, ed. S. Trassati, Elsevier Scientific Publishing Co., 1981.

13. N.V. Kozlova, V.V. Shalaginov, V.N. Lomova, and D.M. Shub, Russian Journal of Inorganic Chemistry, 28, 1395 (1983).

14. C.A. Melendres, and S. Xu, J. Electrochem. Soc., 131, 2239 (1984).

15. V.G. Levich, Physicochemical Hydro-dynamics, Prentice Hall Int'l. Inc. Englewood Cliffs, N.J. (1962).

16. J. Newman, J.Phys. Chem., 70, 1327 (1966).

17. K.E. Gubbins and R.D. Walker, J. Electrochem. Soc., 112, 469 (1965).

18. P. Rasiyah, and A.C.C. Tseung, Electrochemical Society Extended Abstracts, 81-1, pp 1302 - 1307, (1981.)

19. P. Rasiyah, and A.C.C. Tseung, J. Electrochem. Soc., 130, 365 (1983).

20. A.M. Trunov and V.A. Presnov, Elektrokhimiza, 11, 77 (1975).

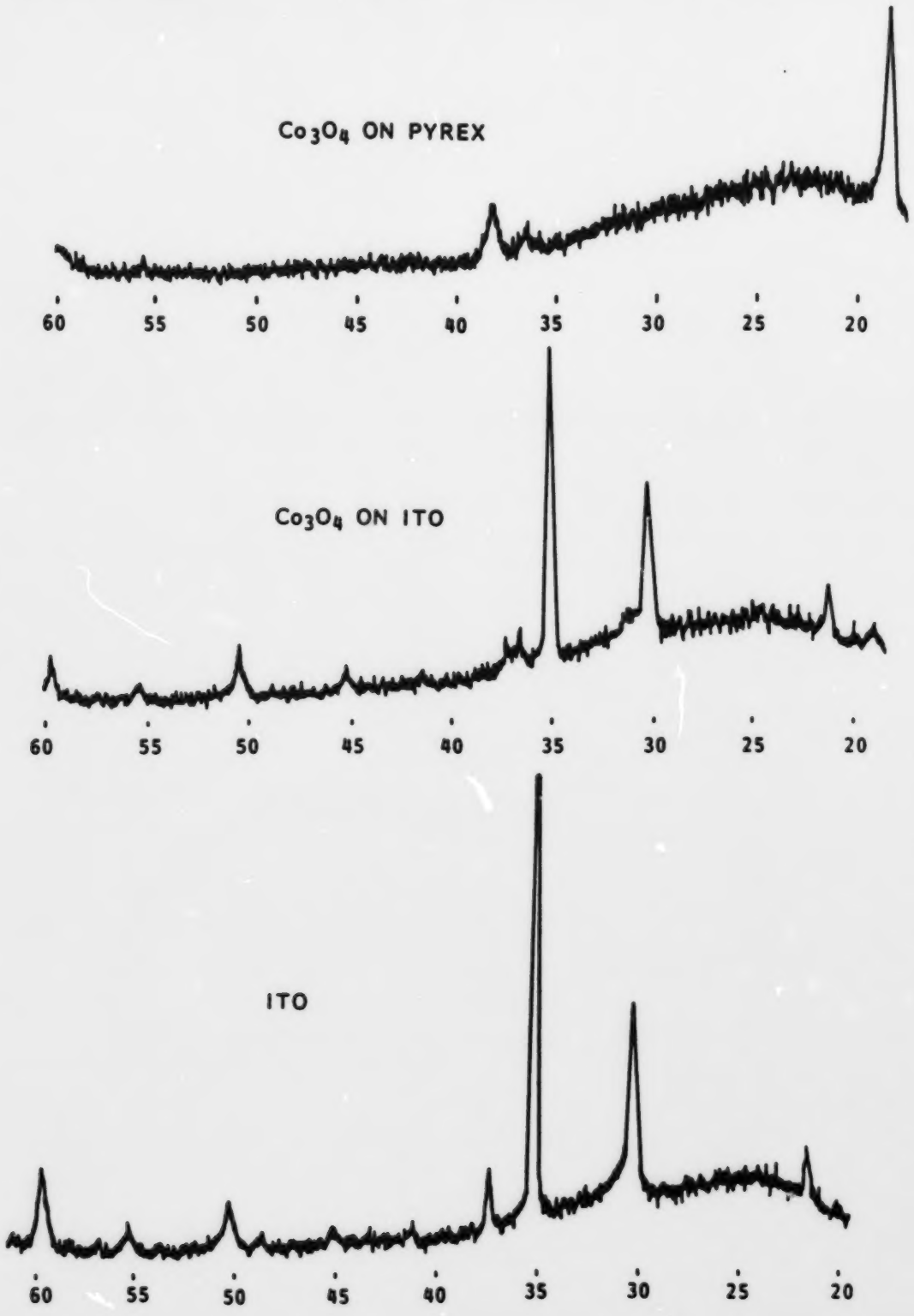

FIGURE 1. X-ray diffraction spectra for a) ~1000 Å cobalt oxide sputter deposited directly onto pyrex, b) ~1000 Å cobalt oxide deposited on ITO and c) ITO on pyrex.

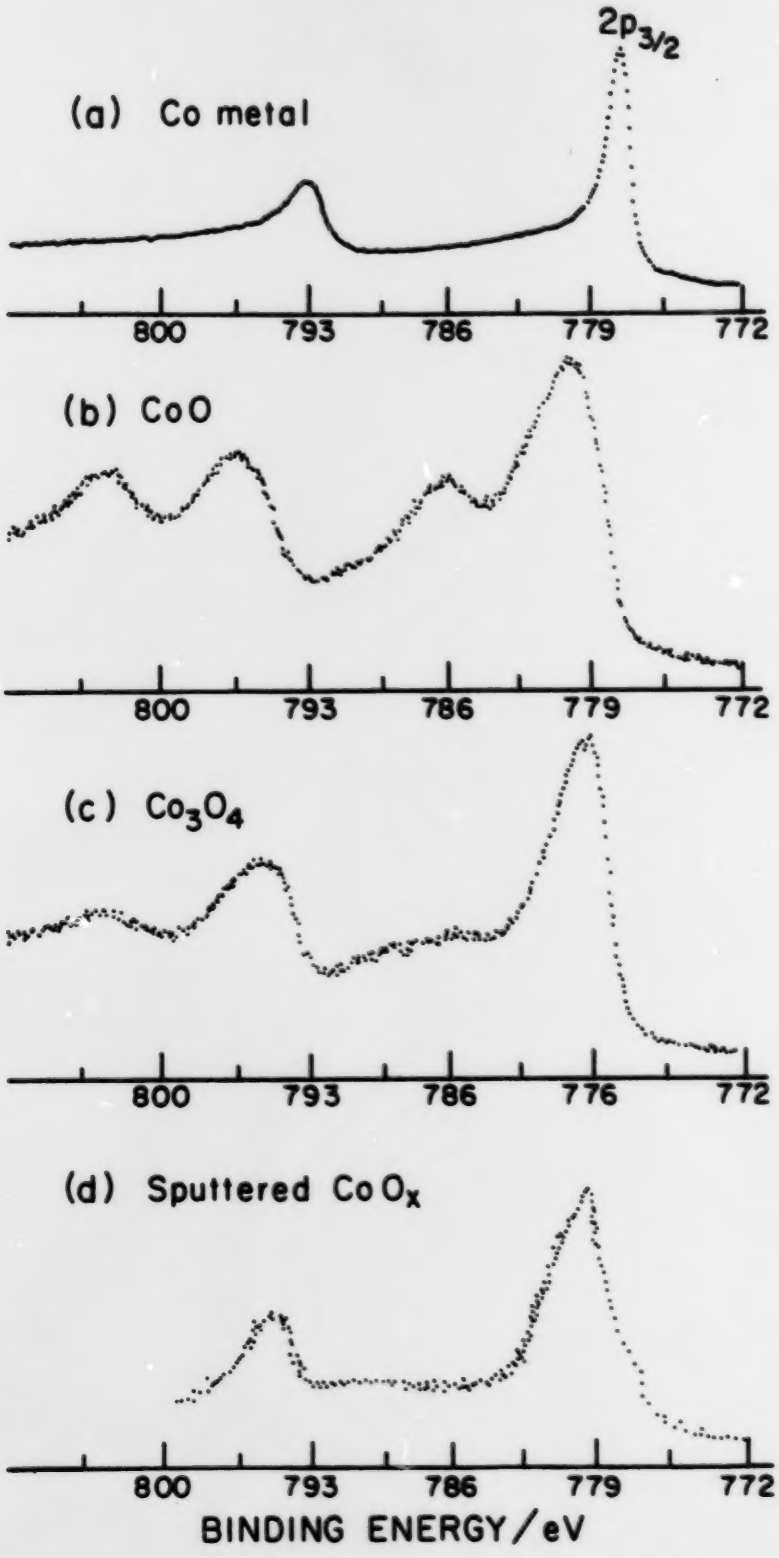

FIGURE 2. XPS spectra of cobalt metal and several cobalt oxide species, from reference 8.

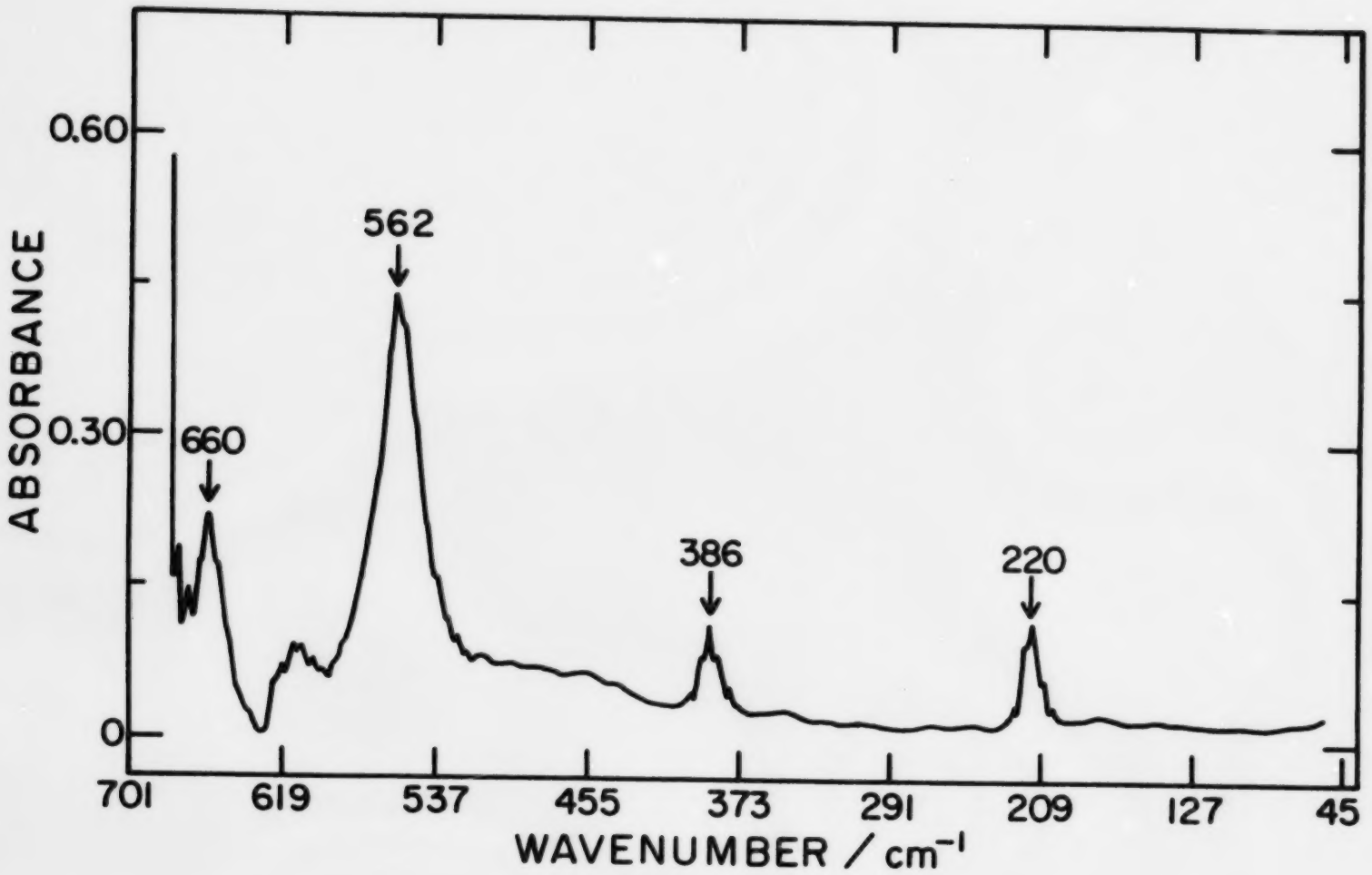

FIGURE 3. Infrared spectrum of ~1000 A cobalt oxide sputter deposited onto silicon substrates.

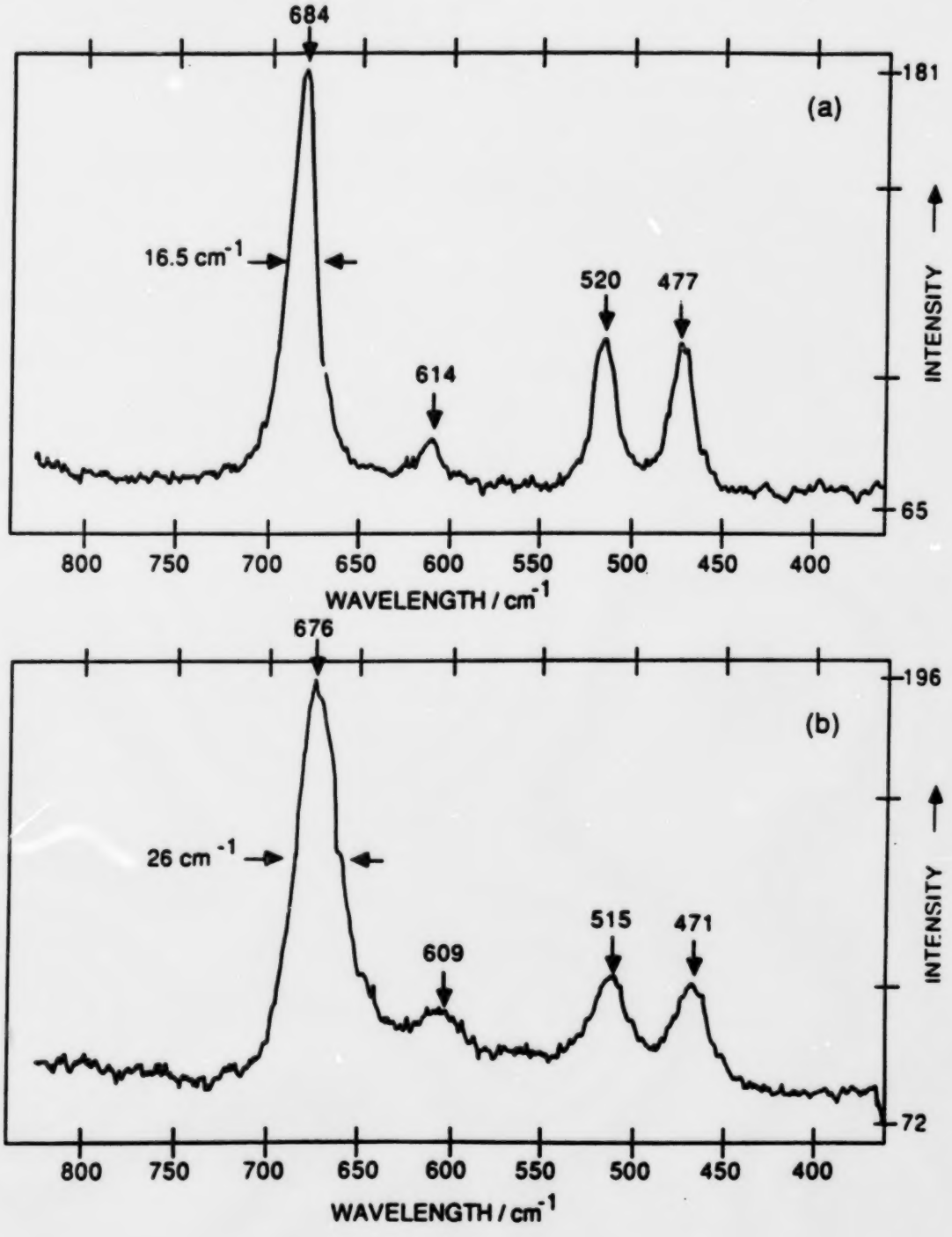

FIGURE 4. Raman spectrum of ~1000 Å cobalt oxide film deposited onto ITO, a) before potential scanning to -0.90 V (SCE) and b) after potential scanning to -0.90 V (SCE).

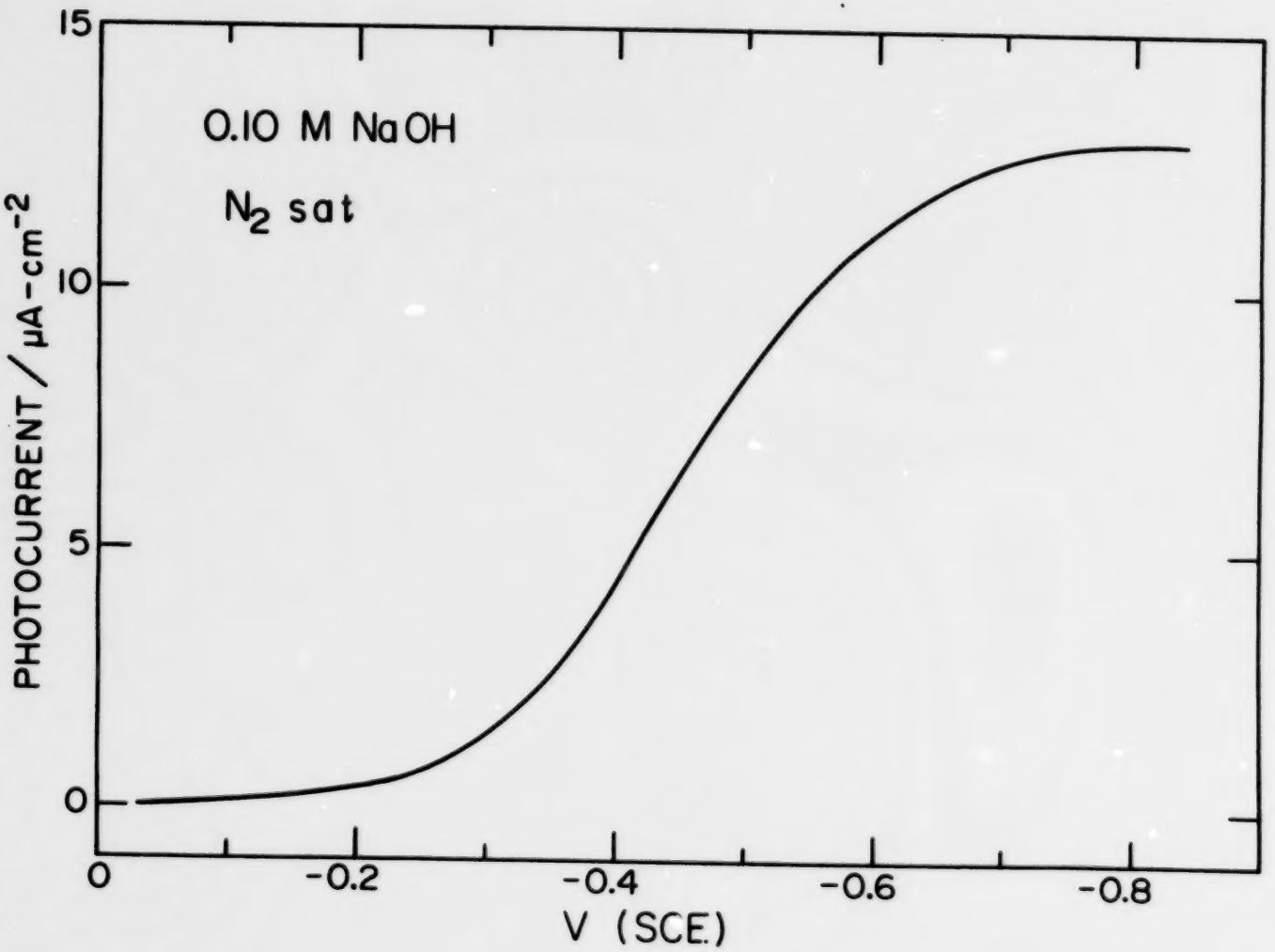

FIGURE 5. AC white light cathodic photoresponse demonstrating p-type semiconducting nature of these cobalt oxide films.

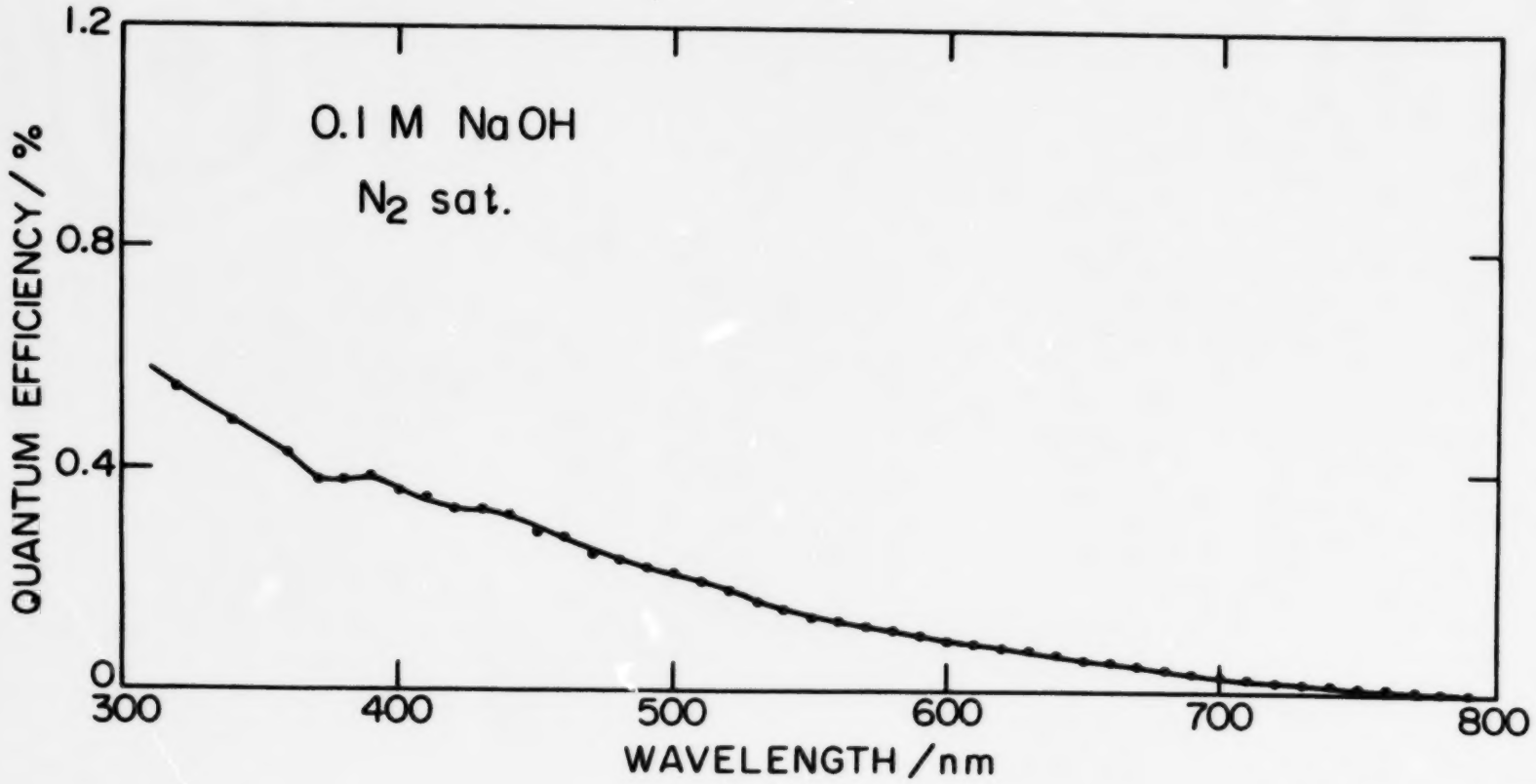

FIGURE 6. AC quantum efficiency measured with electrode held under -0.70 V (SCE) bias.

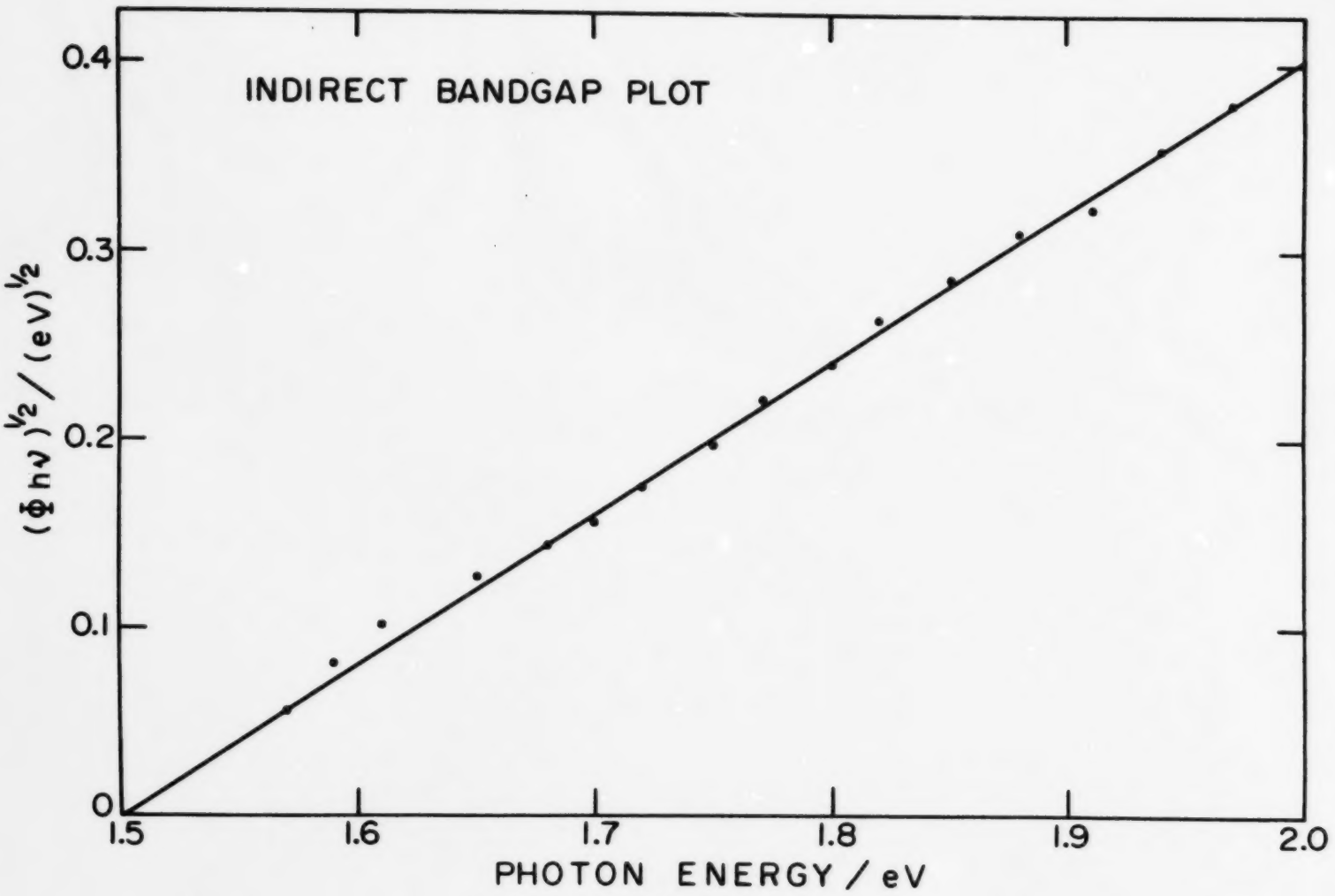

FIGURE 7. Indirect bandgap determination of sputtered cobalt oxide obtained from quantum efficiency data of Fig.6 .

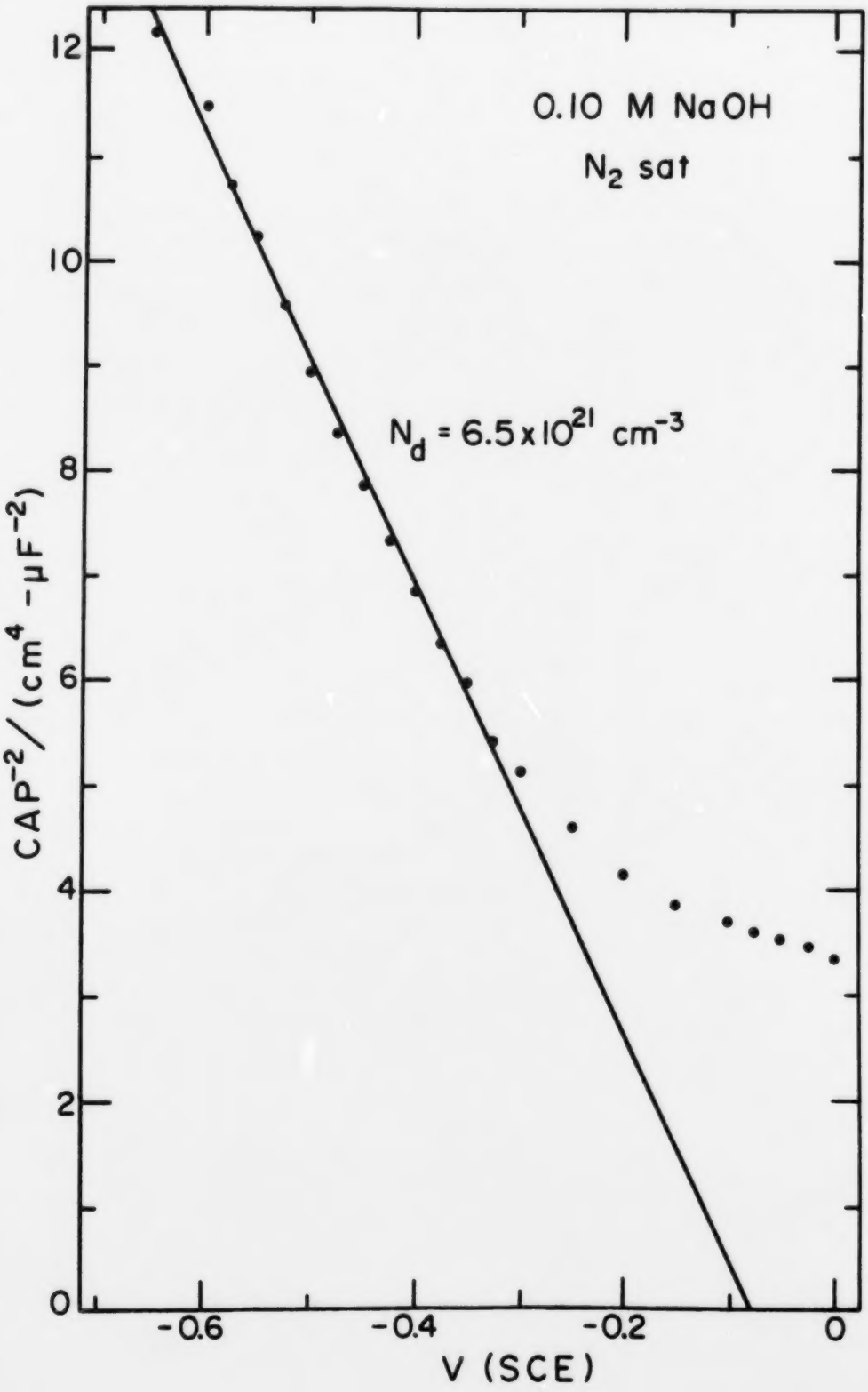

FIGURE 8. Mott-Schottky plot at 10^3 Hz extrapolating to V_{fb} ~ -0.10 V (SCE).

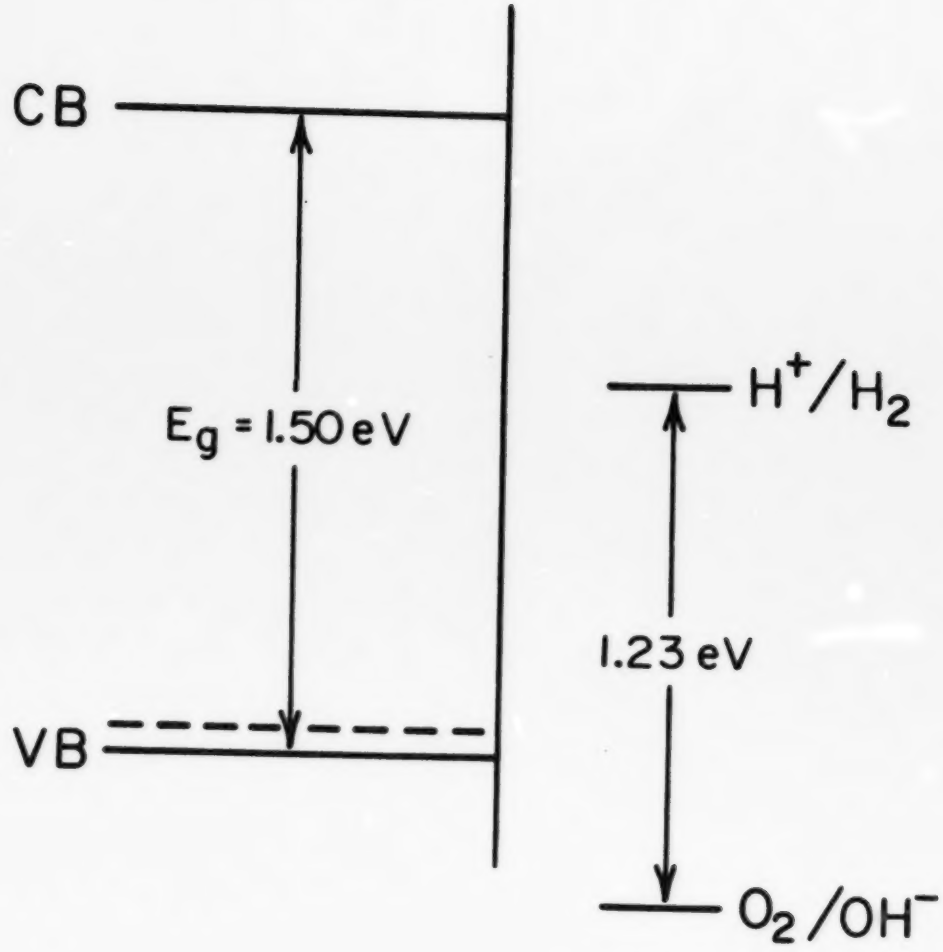

FIGURE 9. Energy level diagram showing the position of the OH^-/O_2 and H^+/H_2 redox levels relative to the conduction and valence bands of the cobalt oxide, constructed using experimentally determined values for E_g and V_{fb}.

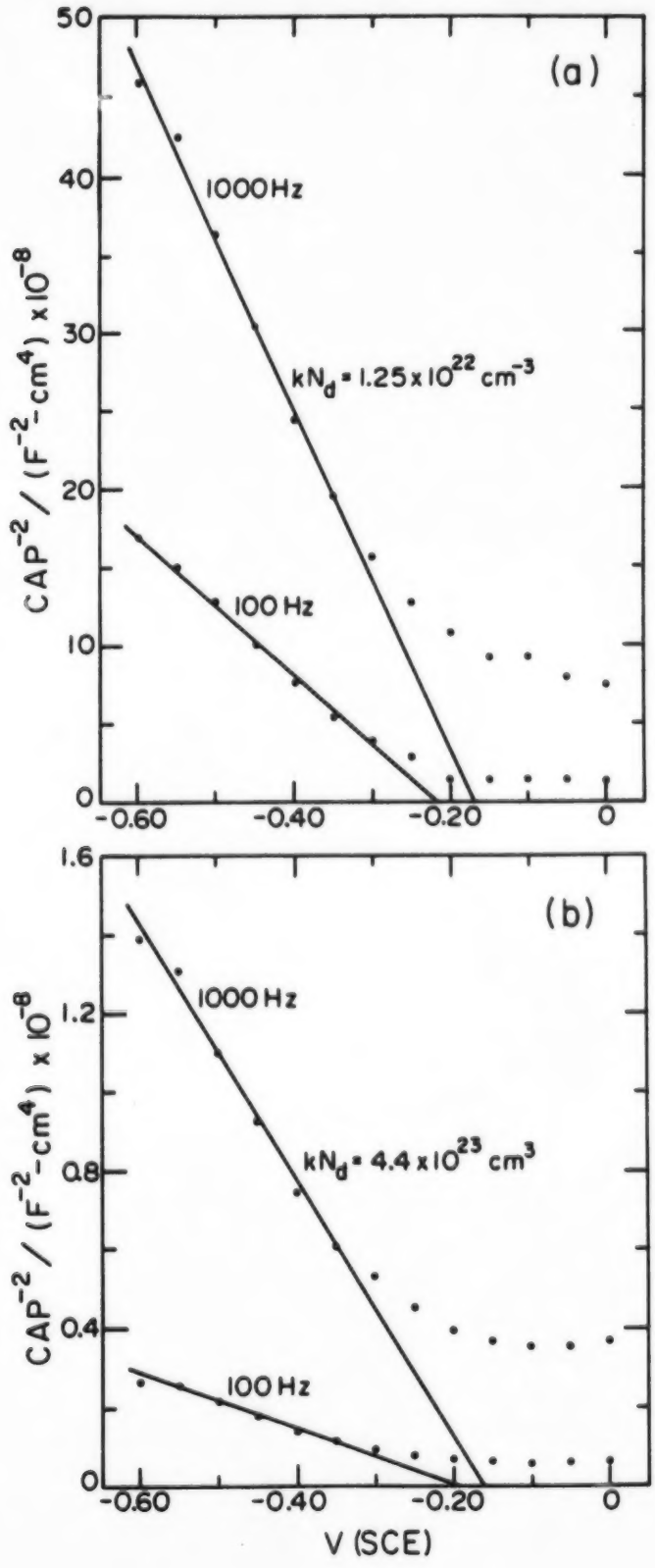

FIGURE 10. Mott-Schottky plots for a) cobalt oxide films deposited and vacuum annealed 8 hours at 300°C and b) cobalt oxide deposited at room temperature.

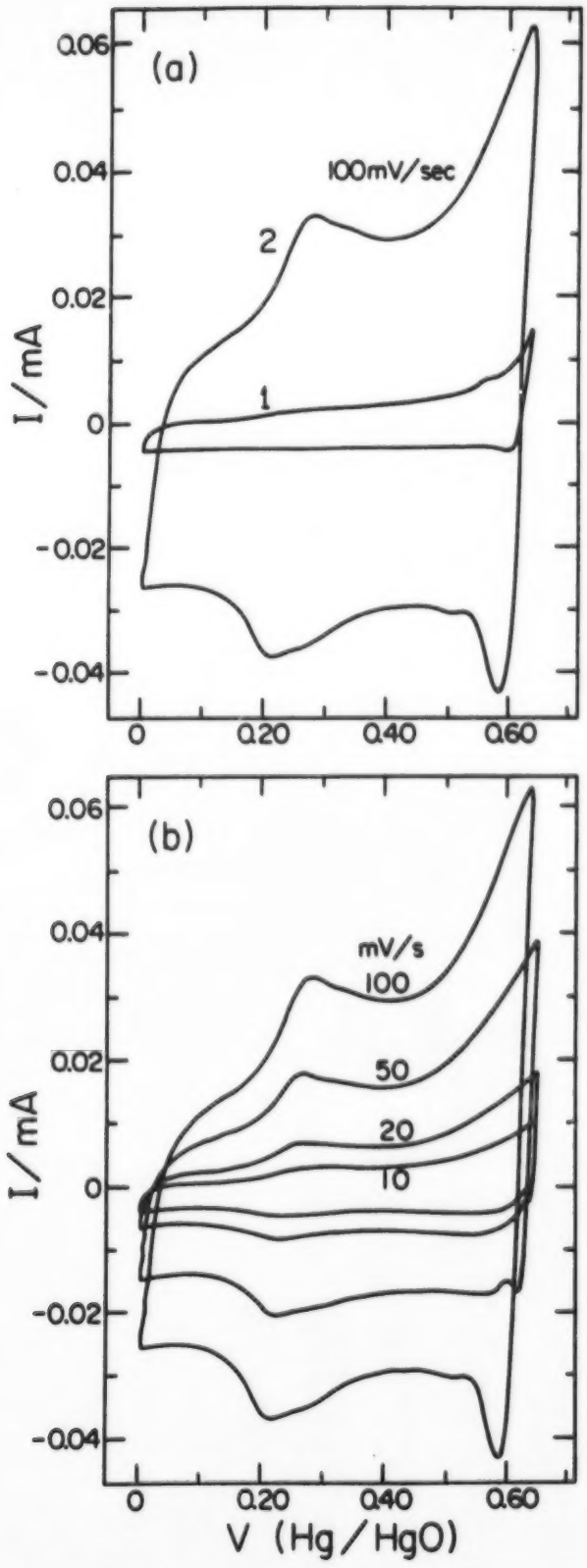

FIGURE 11. Cyclic voltammogram of sputtered cobalt oxide between the potential limits initially a) -0.60 to 0.6 V (Hg/HgO) and then b) after scanning between -0.90 to 0.60 V (Hg/HgO).

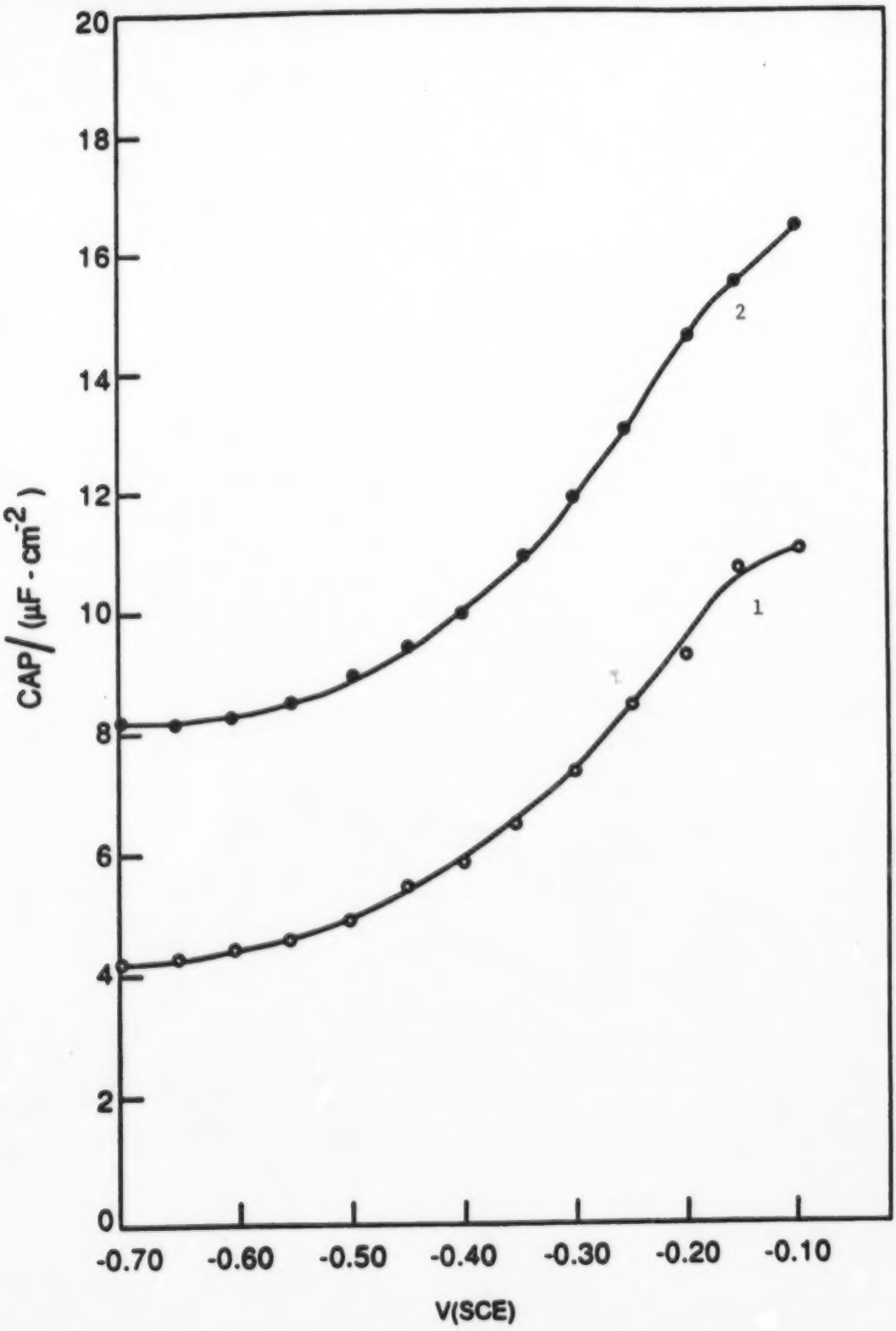

FIGURE 12. Capacitance of electrode of Fig. 11, 1- before and 2- after potential cycling to -0.90 V (Hg/HgO) corresponding to a change from a smooth to rougher morphology film.

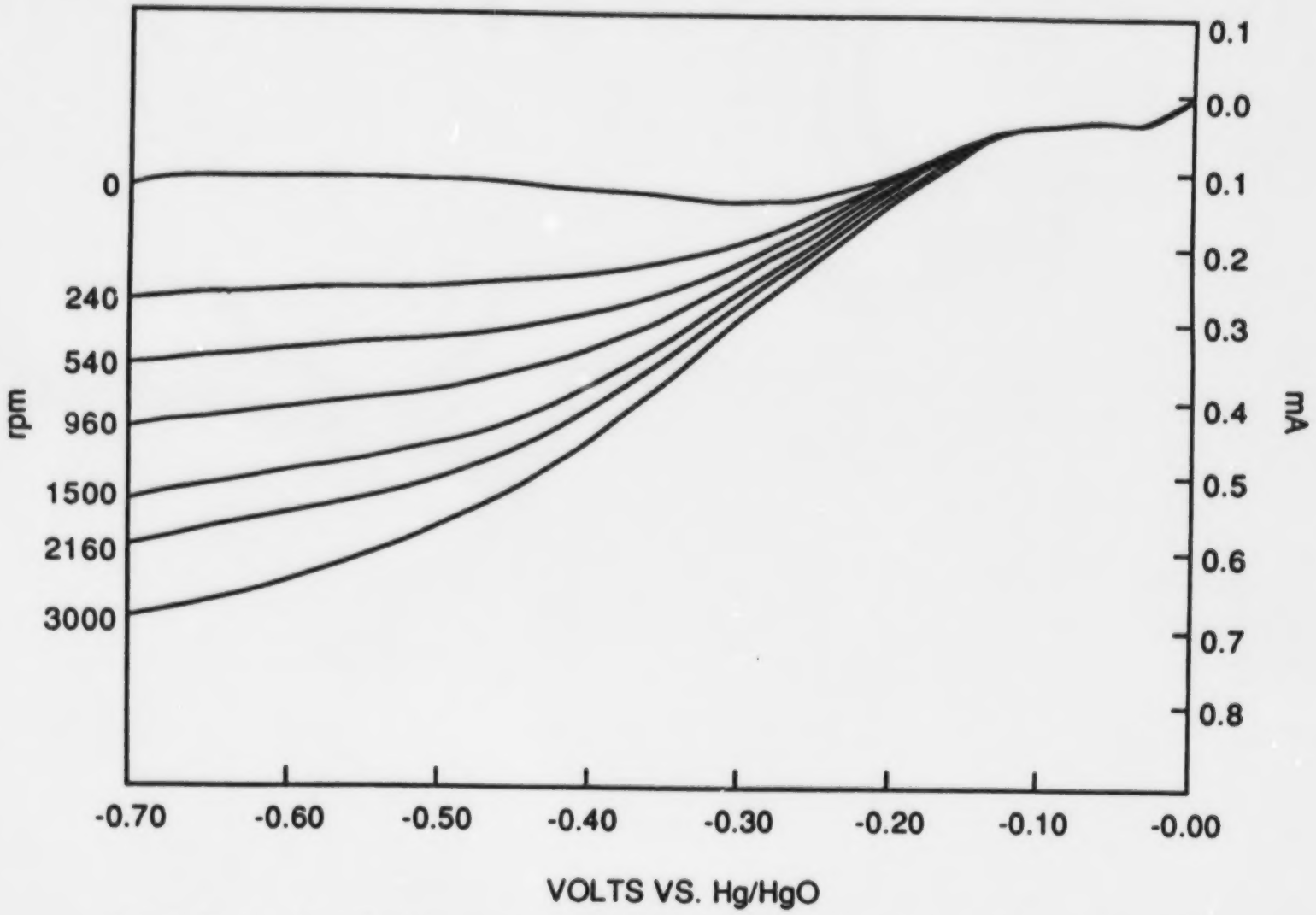

FIGURE 13. O_2 reduction currents at rotating ring disc electrode. Cobalt oxide ~1000 A sputter deposited onto stainless steel disc, area = 0.196 cm^2. Ring current at ~3000 rpm negligible.

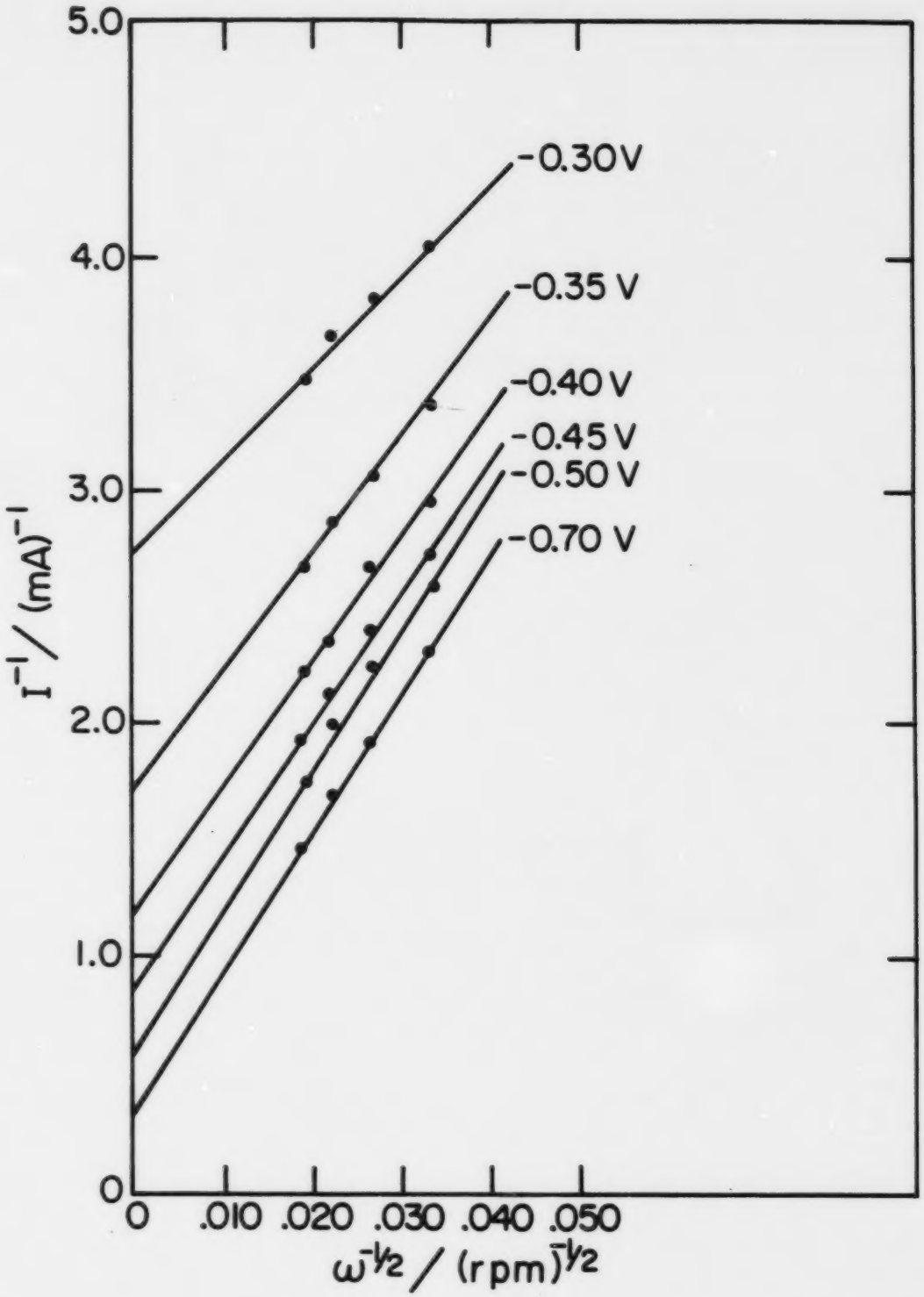

FIGURE 14. Koutecky-Levich plots for cobalt oxide film deposited and vacuum annealed at ~300°C.

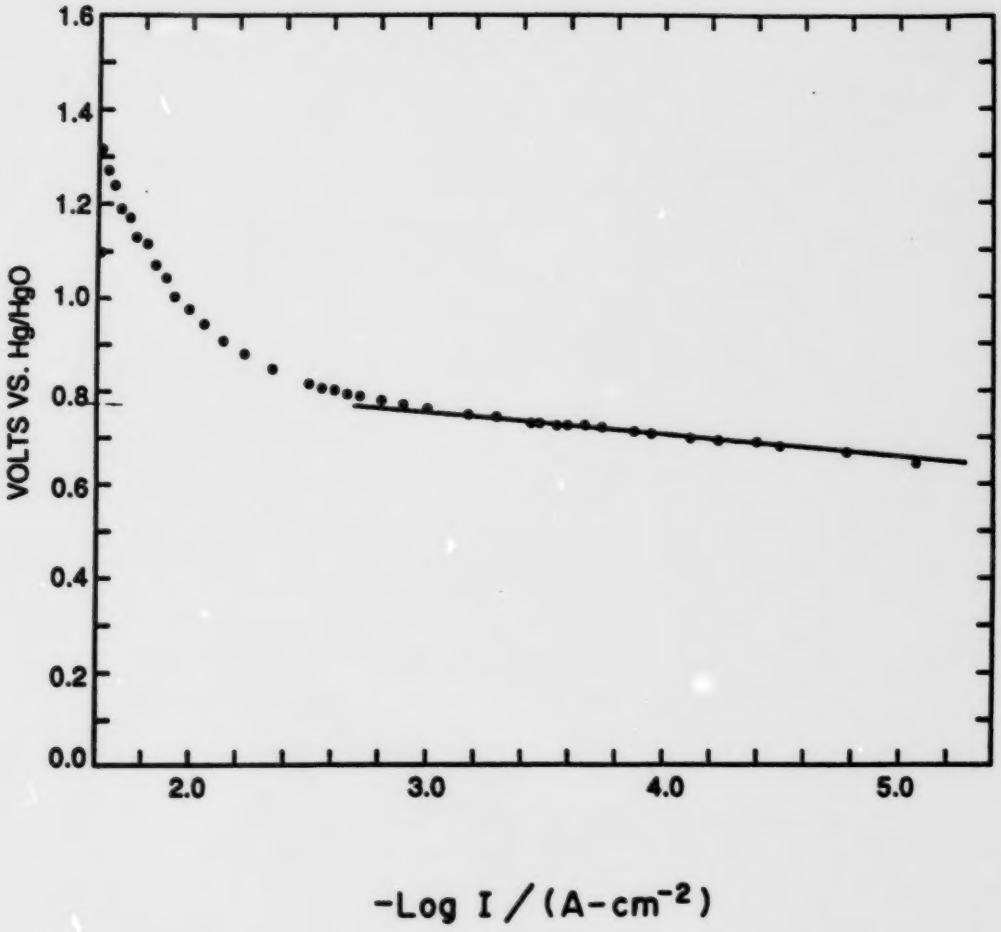

FIGURE 15. Tafel plot for O_2 evolution at room temperature of sputtered cobalt oxide deposited on ITO.